Mugla Journal of Science and Technology

FABRICATION OF MIXED HALIDE PEROVSKITE FILMS BY THERMAL CO-EVAPORATION

Onur Yılmaz

Department of Micro and Nanotechnology, Middle East Technical University, 06800, Ankara, Turkey, syerci@metu.edu.tr
(https://orcid.org/ 0000-0002-9685-1293)

*Selçuk YERCİ**

Department of Micro and Nanotechnology, Department of Electrical and Electronics Engineering, Center for Solar Energy Research and Applications, Middle East Technical University, 06800, Ankara, Turkey, syerci@metu.edu.tr
(https://orcid.org/0000-0003-0599-588X)

Research Article
Received: 21.04.2019, Accepted: 10.06.2019
DOI: 10.22531/muglajsci.556597
*Corresponding author

Abstract

Thermal co-evaporation is a versatile method to fabricate highly uniform, large area and pin-hole free perovskite films for solar cells. In this study, perovskite films ($MAPbI_{3-x}Br_x$) were fabricated entirely by thermal co-evaporation in the full range ($0\leq x\leq 3$) with different Br/I ratio for the first time. Films were characterized optically and structurally using photoluminescence and UV-Vis spectroscopy, X-ray diffraction and scanning electron microscopy. This work presents capability of thermal co-evaporation to fabricate highly-uniform perovskite films at the desired band gaps. $MAPbI_2Br$ film, developed in this study, exhibits no Stokes shift, and therefore is particularly suitable in achieving high efficiency perovskite/silicon tandem solar cells.

Keywords: Band gap tuning, thermal co-evaporation, perovskite

KARIŞIK HALOJENLİ PEROVSKİT FİLMLERİN TERMAL EŞ-BUHARLAŞTIRMA YÖNTEMİ İLE ÜRETİLMESİ

Özet

Perovskit tabakalarının termal eş-buharlaştırma yöntemi ile üretilmeleri güneş hücrelerinde kullanılmak üzere geniş alana sahip, delik kusuru bulunmayan ve homojen filmlerin üretilmesini sağlayan önemli bir tekniktir. Bu çalışmada, tüm aralığı kapsayan ($0\leq x\leq 3$) farklı Br/I oranına dolayısı ile farklı bant aralıklarına sahip $MAPbI_{3-x}Br_x$ perovskit tabakalar eş-buharlaştırma yöntemi ile ilk kez üretilmişlerdir. Geliştirilen filmlerin optik ve yapısal analizleri fotolüminesans, UV-Vis spektrometresi, X-ışını kırınımı ve taramalı elektron mikroskobu ile yapılmıştır. Bu çalışma termal eş-buharlaştırma tekniği ile farklı bant genişliğine sahip homojen perovskit tabakaların elde edilmesinin mümkün olduğunu göstermektedir. Bu çalışmada geliştirilen Stokes kaymasına sahip olmadığı gözlemlenen $MAPbI_2Br$ perovskit filmi, özellikle yüksek verimli perovskit/silisyum çok eklemli güneş hücrelerinin elde edilebilmesi için önemlidir.

Anahtar Kelimeler: Bant aralığı ayarlanabilirliği, termal eş-buharlaştırma, perovskit

Cite

Yılmaz, O., Yerci, S., (2019). "Fabrication of Mixed Halide Perovskite Films By Thermal Co-Evaporation", Mugla Journal of Science and Technology, 5(2), 68-72.

1 Introduction

Since the pioneer work of Kojima et al. in 2009 [1], organic-inorganic halide perovskites have been intensively studied, and reached a certified power conversion efficiency value of 23.7% in 2019 [2]. Among their numerous advantages such as broad absorption [3], long charge diffusion length, high photovoltaic performance and low-cost, the large degree of structural diversity is one of the most important property of ABX_3 perovskite films (A= organic cation, B= divalent metal, and X= halide) [4-6]. Thus, it is possible to tune the band gap of perovskite by altering the A, B or X atoms and/or using multiple cations or anions [7].

Band gap tuning of perovskite films have been widely explored using different fabrication techniques in the literature. In one of the early examples of band gap tuning studies, the single step solution method was used in the fabrication by stoichiometric mixing of $CH_3NH_3PbI_3$ (or simply $MAPbI_3$, which stands for methylamine lead iodide) and $MAPbBr_3$ solutions, and it was concluded that $MAPb(I_{1-x}Br_x)_3$ film at x=0.2 has the enhanced power conversion efficiency and the stability [8]. Using the same deposition method, the importance of the compositional homogeneity of mixed halide perovskites was addressed in a

different study [9]. Band gap tuning of mixed halide perovskites was also investigated using the sequential method. 1M PbI_2 solution in DMF was applied by spin coating and the PbI_2 films were immersed in mixed solutions of MAI and MABr with different volume ratios. This method demonstrated that dipping time as well as the concentrations of the halide solutions has a major impact on the band gap and the composition of the perovskite films [10].

Along with these solution methods, co-evaporation technique is an important alternative for perovskite deposition. It is known that the vacuum depositions are advantageous to fabricate large area, highly uniform and smooth films [11]. Additionally, it is possible to coat perovskite films with a targeted thickness even on relatively rough surfaces [12-14]. Co-evaporation technique was also used to tune the band gap of mixed bromide iodide lead perovskites $MAPb(I_{1-x}Br_x)_3$ (0_x<0.67) thin films using MAI, PbI_2 and $PbBr_2$ precursors. The Br concentration was adjusted by controlling the $PbBr_2$ deposition rate (i.e. controlling the temperature of the $PbBr_2$ crucible) while the deposition rates of the PbI_2 and MAI were kept same during the deposition [15].

In this work, the structural, morphological and optical properties of thermally co-evaporated $MAPbI_{3-x}Br_x$ films with various Br/I ratios in the full range (x is ranging from 0 to 3) were studied systematically for the first time. The nominal bromide content of the perovskite thin films were set beforehand as x equals to 0, 1, 1.33, 2 and 3 in the notation of $MAPbI_{3-x}Br_x$. The chemical reaction formulas of the depositions can be described by the following equations (1-5).

$$x=0:\ MAI + PbI_2 \rightarrow MAPbI_3 \quad (1)$$

$$x=1:\ 2\ MAI + PbI_2 + PbBr_2 \rightarrow MAPbI_2Br \quad (2)$$

$$x=1.33:\ 3\ MAI + PbI_2 + 2\ PbBr_2 \rightarrow MAPbI_{1.67}Br_{1.33} \quad (3)$$

$$x=2:\ 2\ MABr + PbI_2 + PbBr_2 \rightarrow MAPbIBr_2 \quad (4)$$

$$x=3:\ MABr + PbBr_2 \rightarrow MAPbBr_3 \quad (5)$$

The results clearly demonstrate the band gap widening and lattice space decreasing with increasing Br^- concentration. $MAPbI_2Br$ film with a band gap of 1.65 eV, which is suitable for tandem solar cells was fabricated with no Stokes shift determined from PL and UV-Vis spectroscopies.

2 Materials and Methods

Unless otherwise stated, all chemicals were purchased from commercial sources and used without further purification. Perovskite depositions were made in ambient atmosphere (30% relative humidity [RH] and 26-30°C) on glass substrates. Lead iodide (PbI_2, 99.999%) and lead bromide ($PbBr_2$, 99.999%) powders were obtained from Sigma-Aldrich. Surface morphology of the perovskite films were investigated by Quanta 400F Scanning Electron Microscope. Structural analyses were conducted at room temperature in 2Θ scan range of 10°- 45° with Rigaku Miniflex X-Ray diffractometer using Cu K_α (0.154 nm) radiation. Transmission and reflection spectra were measured using a home-built system equipped with an integrating sphere. The photoluminescence spectrum were recorded using MS257 monochromator. A laser centered at 532 nm is used to excite the perovskite samples, except a laser operating at 325 nm is used to excite the $MAPbBr_3$ sample due to its large band gap.

2.1 Syntheses of methylammonium iodide (MAI) and methylammonium bromide (MABr)

30 mL of methylamine (40% in methanol, TCI) and 32.3 mL of hydroiodic acid or 23.3 mL of hydrobromic acid (48% in deionized water) were placed in a round bottom flask and stirred for 2 hours at 0°C. Solvents were evaporated at 50°C during 1 hour. Crude products were dissolved in ethanol and recrystallized from diethyl ether. After several washing with diethyl ether, MAI and MABr crystals were dried at 60°C in air.

2.2 Deposition of perovskite layers

Glass substrates were cleaned by sequential ultrasonication in Hellmanex, deionized water, acetone and isopropyl alcohol and exposed to UV-ozone for 15 minutes just before the coating process. As shown in Table 1, substrates were coated by varying the evaporation temperatures of the individual precursors to adjust the desired stoichiometry. $MAPbI_3$ and $MAPbBr_3$ films were deposited using their corresponding precursors. PbI_2 and MAI were loaded into two separate boron nitride crucibles in the chamber (Vaksis R&D) to obtain $MAPbI_3$, whereas $PbBr_2$ and MABr were used for $MAPbBr_3$ deposition. The deposition rates of the organic cations were maintained at 0.5 $Å.s^{-1}$, while the rates of the inorganic halides were kept at 0.3 $Å.s^{-1}$ under 3.0 x 10^{-5} Torr deposition pressure. During deposition of $MAPbI_2Br$, $MAPbI_{1.67}Br_{1.33}$ and the $MAPbIBr_2$ films, all three of the sources in the evaporation chamber were used simultaneously. Temperature of the crucibles of $PbBr_2$, MAI and PbI_2 were kept at 325°C (0.3 $Å.s^{-1}$), 200°C (0.6 $Å.s^{-1}$) and 285°C (0.3 $Å.s^{-1}$) to prepare the $MAPbI_2Br$ film. The $MAPbI_{1.67}Br_{1.33}$ stoichiometry was achieved using a $PbBr_2$ deposition rate of 0.4 $Å.s^{-1}$ a PbI_2 deposition rate of 0.2 $Å.s^{-1}$. Lastly, MABr was used instead of MAI while keeping the temperature of the crucible at 230°C (0.6 $Å.s^{-1}$) to deposit the $MAPbIBr_2$ film by keeping the rates of $PbBr_2$ and PbI_2 as 0.3 $Å.s^{-1}$. Perovskite film thicknesses were around 300 nm for all depositions by controlling deposition time.

3 Results and Discussion

3.1 Vacuum co-evaporation method

Illustration of the three-sourced thermal co-evaporation of the perovskite films is given in Figure 1. Source materials were replaced with fresh ones in the beginning of each coating process. After each deposition, perovskite films were annealed at ambient atmosphere (~30% relative humidity, 100 °C) for 10 minutes to enhance the crystallization. At least 8 samples were prepared for each stoichiometry for characterizations.

Table 1. Fabrication details (temperature of crucibles, deposition rate of source materials and diffusion pump valve opening ratios) of co-evaporated $MAPb(I_{1-x}Br_x)_3$ films.

Ratio	Source 1			Source 2			Source 3			Diffusion valve opening
	Material	Temp. (°C)	Rate (Å/s)	Material	Temp. (°C)	Rate (Å/s)	Material	Temp. (°C)	Rate (Å/s)	
x=0	-	-	-	MAI	195	0.5	PbI_2	285	0.3	24%

x=1	$PbBr_2$	325	0.3	MAI	200	0.6	PbI_2	285	0.3	20%
x=1.33	$PbBr_2$	335	0.4	MAI	190	0.6	PbI_2	280	0.2	16%
x=2	$PbBr_2$	320	0.3	MABr	230	0.6	PbI_2	285	0.3	16%
x=3	$PbBr_2$	320	0.3	MABr	230	0.5	-	-	-	30%

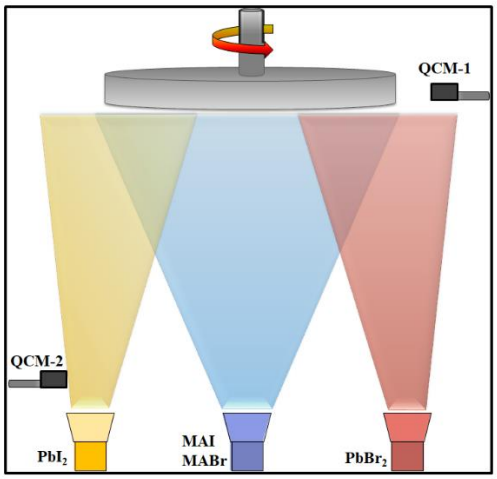

Figure 1. Three-sourced vacuum co-evaporation of perovskite films.

Figure 2 shows the optical images $MAPbI_{3-x}Br_x$ ($0 \le x \le 3$) films on glass. A color transition from dark brown to orange and yellow with increasing Br content (i.e. increasing x in the stoichiometry) indicates the increasing band gap of the perovskite films.

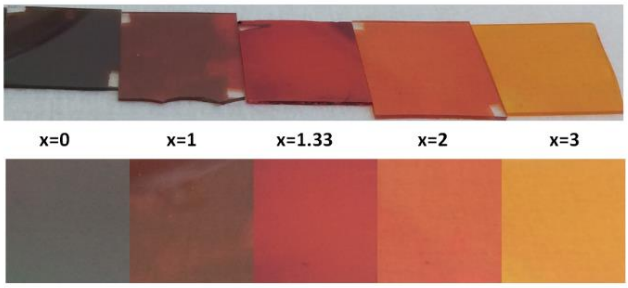

Figure 2. Optical images of evaporated $MAPbI_{3-x}Br_x$ films (top), color transition of evaporated $MAPbI_{3-x}Br_x$ films (bottom).

3.2 Structural and morphological characterization

Figure 3a shows the XRD patterns of $MAPbI_{3-x}Br_x$ ($0 \le x \le 3$). A systematic change was monitored from the tetragonal structure of $MAPbI_3$ to the cubic structure of $MAPbBr_3$ [1, 8, 16, 17]. Two peaks of $MAPbI_3$ located at 14.15° and 28.40° are associated with the (110)t and (220)t crystal planes, respectively. As seen in diffractograms, replacement of I with Br in $MAPbI_{3-x}Br_x$ film caused the transforming of (110)t peak into (100)c peak, while (220)t peak into (200)c peak. With increasing Br content, gradual shifts were monitored for peaks diffracted by the (100)c and (200)c planes toward higher 2Θ degrees due to decreasing lattice spacing with smaller Br^- ions.

The average crystallite size of the perovskite films were estimated according to Scherrer's equation using the full width at half maximum (FWHM) values (Figure 3b) of the peaks originated from (110)t and (100)c planes [18-20]. Fractional differences were observed in grain sizes resulting from the inherent local variations of halides in lattice positions. They were calculated as 29.53 nm, 26.97 nm, 18.57 nm, 24.26 nm, and 25.74 nm in the order of increasing Br content.

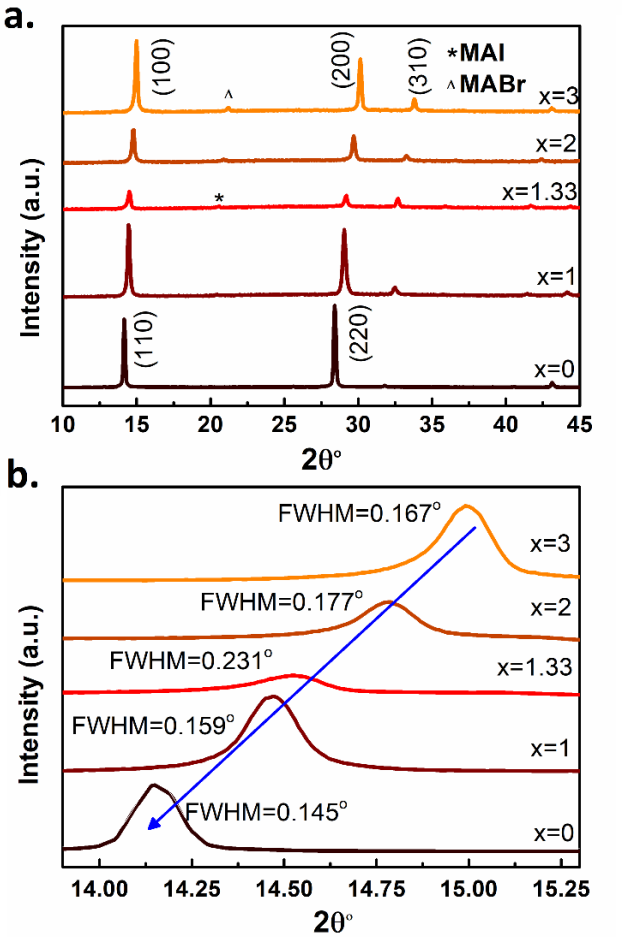

Figure 3. (a) XRD patterns of perovskite films (b) Detailed scans of the (110)t and (100)c crystal orientations.

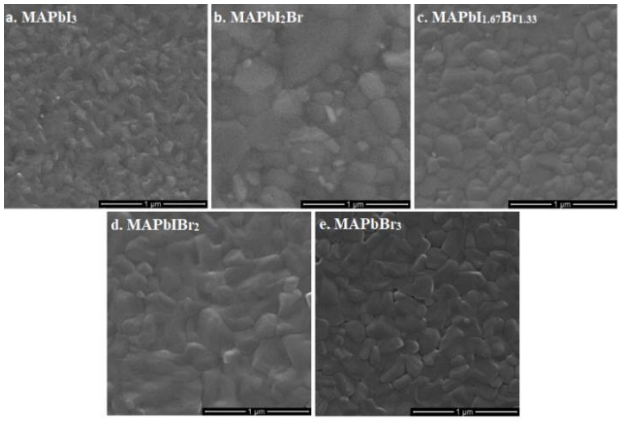

Figure 4. SEM images of co-evaporated perovskite films (a) $MAPbI_3$ (b) $MAPbI_2Br$ (c) $MAPbI_{1.67}Br_{1.33}$ (d) $MAPbIBr_2$ and (e) $MAPbBr_3$.

Figure 4 shows the scanning electron microscopy (SEM) images of the co-evaporated perovskite films. Films with all compositions have a complete coverage of glass surfaces, and they are pinhole free and homogeneous. The most apparent difference was observed for the $MAPbI_3$ film which has a preferential crystal orientation of (110)t. Films with Br incorporation typically have larger crystal grains at the top surface of the films with a maximal for the $MAPbI_2Br$ film.

3.3 Optical analysis

Absorption spectra of co-evaporated perovskite films on glass substrates were recorded to monitor their optical responses. The corresponding gradual shift in the absorption band edges, illustrated in Figure 5a, provides further confirmation that Br has successfully incorporated to the $MAPbI_{3-x}Br_x$ ($0 \le x \le 3$) films by the co-evaporation. The absorption onset value shifts systematically from 810 nm ($MAPbI_3$) to 580 nm ($MAPbBr_3$) with increasing MABr content. The optical band gap of $MAPbI_{3-x}Br_x$ films were calculated in the range between 1.55 eV and 2.3 eV using the Tauc plots (Figure 5b), which are consisted with the earlier reports in the literature [8], and demonstrating that band gap of $MAPbI_{3-x}Br_x$ can be controlled by co-evaporation of MAI/MABr, PbI_2 and $PbBr_2$.

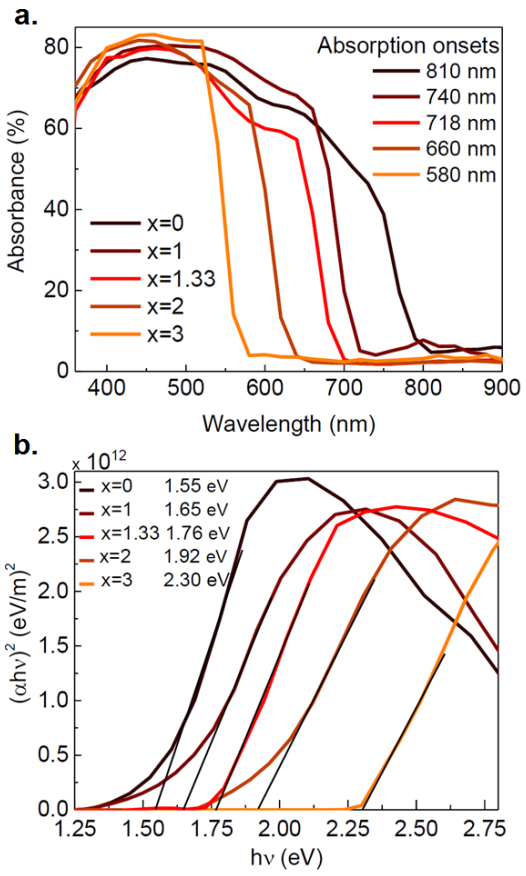

Figure 5. (a) Absorption spectra of perovskite films (b) Tauc plots of perovskite films having different band gap values.

Figure 6 shows the photoluminescence spectra of co-evaporated $MAPbI_{3-x}Br_x$ ($0 \le x \le 3$) films with different x values. The PL signal peaks at wavelengths located in between 533 nm and 801 nm for x=0 and x=3, respectively. A clear blue-shift of the PL peak position with Br incorporation is observed. Under 532 nm and 325 nm excitations, we observed no decomposition (i.e. formation of multiple PL peaks) of the films, indicating films are mostly homogenous in composition.

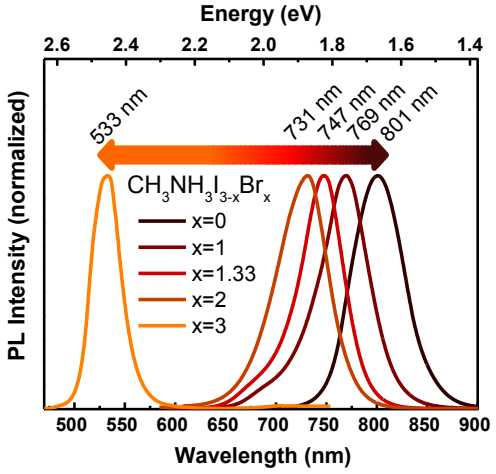

Figure 6. Normalized PL peaks of the $MAPbI_{3-x}Br_x$ films.

The comparison of the optical band gap values obtained from the Tauc-plots and the PL peaks are given in Figure 7. As shown in the figure, band gap values differ nearly ~0.1 eV and ~0.2 eV for the $MAPbI_{1.67}Br_{1.33}$ and $MAPbIBr_2$, respectively. These discrepancies can be attributed to the halide migration and/or the lattice relaxation [9]. On the other hand, the $MAPbI_2Br$ mixed halide perovskite showed a very small shift in its optical band gap values which were calculated as 1.65 eV from the Tauc plot and 1.61 eV from its PL peak. This small difference indicates the co-evaporation of PbI_2, $PbBr_2$ and MAI resulted in a single phase perovskite film with a band gap suitable for tandem solar cell applications.

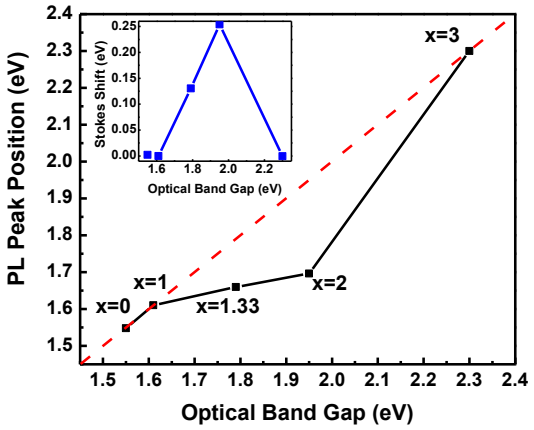

Figure 7. Comparison of the band gap values of $MAPbI_{3-x}Br_x$ ($0 \le x \le 3$) films.

4 Conclusion

Co-evaporation of PbI_2, $PbBr_2$ and MAI/MABr allowed us to study the effect of Br/I ratio on morphological and optical properties of perovskite layers more systematically and reliably. Five sets of pin-hole free and homogenous $MAPbI_{3-x}Br_x$ ($0 \le x \le 3$) perovskite films with different shades of brown and orange colors were successfully fabricated on glass substrates. Gradual shifts of the XRD peaks toward higher $2\Theta°$ observed with the increasing amount of relatively small Br^- ions. Our results showed that, it is possible to tune the band of the mixed halide perovskite in the full range of Br/I ratio. We have achieved to fabricate $MAPbI_2Br$ mixed halide perovskite with a band gap of 1.65 eV and negligibly-small Stokes shift, suitable for perovskite/silicon tandem solar cells.

5 Acknowledgment

This work was supported by the Scientific and Technological Research Council of Turkey (TÜBİTAK), Grant No: 114F306. S.Y. would like to offer his special thanks to Wiria Soltanpoor for his help in fabrication and characterization of perovskite films.

6 References

[1] Kojima, A., Teshima, K., Shirai, Y. and Miyasaka, T., "Organometal Halide Perovskites as Visible-Light Sensitizers for Photovoltaic Cells", *Journal of the American Chemical Society,* 131(17), 6050-6051, 2009.

[2] https://www.nrel.gov/pv/cell-efficiency.html

[3] Kim, H.S., Lee, C.R., Im, J.H., Lee, K.B., Moehl, T., Marchioro, A., Moon, S.J., Humphry-Baker, R., Yum, J.H., Moser, J.E. Grätzel, M. and Park, N.G., "Lead Iodide Perovskite Sentisized All-Solid-State Submicron Thin Film Mesoscopic Solar Cell with Efficiency Exceeding 9%", *Scientific Reports*, 2(591), 1–7, 2012.

[4] Chen, W., Wu, Y., Yue, Y., Liu, J., Zhang, W., Yang, X., Chen, H., Bi, E., Ashraful, I., Grätzel, M. and Han, L., "Efficient and Stable Large-Area Solar Cells with Inorganic Charge Extraction Layers", *Science,* 350, 944–948, 2015.

[5] Shi, D., Adinolfi, V., Comin, R., Yuan, M., Alarousu, E., Buin, A., Chen, Y., Hoogland, S., Rothenberger, A., Katsiev, K., Losovyj, Y., Zhang, X., Dowben, P., Mohammed, O., Sargent E. and Bakr O., "Low Trap-State Density and Long Carrier Diffusion in Organolead Trihalide Perovskite Single Crystals", *Science,* 347, 519–522, 2015.

[6] Cao, K., Li, H., Liu, S.S., Cui, J., Shen Y. and Wang, M., "$MAPbI_{3-x}Br_x$ Mixed Halide Perovskites for Fully Printable Mesoscopic Solar Cells with Enhanced Efficiency and Less Hysteresis", *Nanoscale,* 8, 8839-8846, 2016.

[7] Sahli, F., Werner, J., Kamino, B.A., Brauninger, M., Monnard, R., Paviet-Salomon, B., Barraud, L., Ding, L., Leon, J.J.D., Sacchetto, D., Cattaneo, G., Despeisse, M., Boccard, M., Nicolay, S., Jeangros, Q., Niesen, B. and Ballif, C. "Fully Textured Monolithic Perovskite/Silicon Tandem Solar Cells with 25.2% Power Conversion Efficiency", *Nature Materials,* 17, 820–826, 2018.

[8] Noh, J.H., Im, S.H., Heo, J.H., Mandal, T.N. and Seok, S.I., "Chemical Management for Colorful, Efficient, and Stable Inorganic–Organic Hybrid Nanostructured Solar Cells", *Nano Letters,* 13, 1764–1769, 2013.

[9] Sadhanala, A., Deschler, F., Thomas, T.H., Dutton, S.E., Goedel, K.C., Hanusch, F.C., Lai, M.L. Steiner, U., Bein, T. Docampo, P., Cahen, D. and Friend, R.H., "Preparation of Single-Phase Films of $CH_3NH_3Pb(I_{1-x}Br_x)_3$ with Sharp Optical Band Edges", *The Journal of Physical Chemistry Letters,* 5, 2501–2505, 2014.

[10] Kulkarni, S.A., Baikie, T., Boix, P.P., Yantara, N., Mathews N. and Mhaisalkar, S., "Band-Gap Tuning of Lead Halide Perovskites Using a Sequential Deposition Process", *Journal of Materials Chemistry A,* 2, 9221–9225, 2014.

[11] Liang G., Lan H., Fan, P., Lan, C., Zheng, Z., Peng, H. and Luo, J., "Highly Uniform Large-Area (100 cm^2) Perovskite $CH_3NH_3PbI_3$ Thin-Films Prepared by Single-Source Thermal Evaporation", *Coatings,* 8, 256(1-11), 2018.

[12] Liu, M., Johnston, M.B. and Snaith, H.J., "Efficient Planar Heterojunction Perovskite Solar Cells by Vapour Deposition", *Nature,* 501, 395–398, 2013.

[13] McMeekin, D.P., Sadoughi, G., Rehman, W., Eperon, G.E., Saliba, M., Hörantner, M.T., Haghighirad, A., Sakai, N., Korte, L., Rech, B., Johnston, M.B., Herz, L.M. and Snaith, H.J., "A Mixed-Cation Lead Mixed-Halide Perovskite Absorber for Tandem Solar Cells", *Science,* 351, 151–155, 2016.

[14] Eperon, G. E., Leijtens, T., Bush, K.A., Prasanna, R., Green, T., Wang, J.T.-W., McMeekin, D.P., Volonakis, G., Milot, R.L., May, R., Palmstrom, A., Slotcavage, D.J, Belisle, R.A., Patel, J.B., Parrott, E.S., Sutton, R.J., Ma, W., Moghadam, F., Conings, B., Babayigit, A., Boyen, H.-G., Bent, S., Giustino, F., Herz, L.M., Johnston, M.B., McGehee, M.D. and Snaith, H.J., "Perovskite-Perovskite Tandem Photovoltaics with Optimized Band Gaps", *Science,* 354, 861–865, 2016.

[15] Zhou, X., Ye, W., Li, X., Zheng, W., Lin, R., Huang, F. and Zhong, D., "Band Alignment of $MAPb(I_{1-x}Br_x)_3$ Thin Films by Vacuum Deposition", *Applied Physics Letters,* 109, 233906(1-4), 2016.

[16] Im, J.-H., Lee, C.-R., Lee, J.-W, Park, S.-W. and Park, N.-G. "6.5% Efficient Perovskite Quantum-Dot-Sensitized Solar Cell", *Nanoscale,* 3, 4088–4093, 2011.

[17] Baikie, T., Fang, Y., Kadro, J.M., Schreyer, M., Wei, F., Mhaisalkar, S.G., Gratzel, M. and White, T.J., "Synthesis and Crystal Chemistry of the Hybrid Perovskite $(CH_3NH_3)PbI_3$ for Solid-State Sensitised Solar Cell Applications", *Journal of Materials Chemistry A,* 1, 5628–5641, 2013.

[18] Hu, Y., Schlipf, J., Wussler, M., Petrus, M.L., Jaegermann, W., Bein, T. Müller-Buschbaum, P. and Docampo, P., "Hybrid Perovskite/Perovskite Heterojunction Solar Cells" *ACS Nano,* 10, 5999–6007, 2016.

[19] Patterson, A.L., "The Scherrer Formula for X-Ray Particle Size Determination", *Physical Review,* 56, 978-982, 1939.

[20] Wang, K., Lin, Z., Ma, J., Liu, Z., Zhou, L., Du, J., Chen, D., Zhang, C., Chang, J. and Hao, Y., "High-Performance Simple-Structured Planar Heterojunction Perovskite Solar Cells Achieved by Precursor Optimization", *ACS Omega,* 2, 6250–6258, 2017.